

1 **HaloTag is an effective expression and solubilisation fusion partner for a range of**  
2 **fibroblast growth factors**

3 Changye Sun<sup>1,2</sup>, Yong Li<sup>1,2</sup>, Sarah Taylor<sup>1</sup>, Xianqing Mao<sup>3</sup>, Mark C. Wilkinson<sup>1</sup>, David G.  
4 Fernig<sup>1,2</sup>

5 <sup>1</sup>Department of Biochemistry, Institute of Integrative Biology, University of Liverpool,  
6 Liverpool L69 7ZB, UK; <sup>3</sup>Laboratory of Cellular and Molecular Oncology, Centre de  
7 Recherche Public de la Santé (CRP-Santé), 84, Val Fleuri, L-1526 Luxembourg.

8  
9 <sup>2</sup>Corresponding authors:

10 Changye Sun, Yong Li, David G. Fernig

11 Department of Biochemistry, Institute of Integrative Biology, University of Liverpool,  
12 Liverpool L69 7ZB, UK

13 Tel. +44 151 795 4471

14 E. hscsun@liv.ac.uk, Y.li47@liv.ac.uk, dgfernig@liv.ac.uk

15

16 **Abstract:**

17 The production of recombinant proteins such as the fibroblast growth factors (FGFs) is the  
18 key to establishing their function in cell communication. The production of recombinant  
19 FGFs in *E.coli* is limited, however, due to expression and solubility problems. HaloTag has  
20 been used as a fusion protein to introduce a genetically-encoded means for chemical  
21 conjugation of probes. We have expressed 11 FGF proteins with an N-terminal HaloTag,  
22 followed by a tobacco etch virus (TEV) protease cleavage site to allow release of the FGF  
23 protein. These were purified by heparin-affinity chromatography, and in some instances by  
24 further ion-exchange chromatography. It was found that HaloTag did not adversely affect the  
25 expression of FGF1 and FGF10, both of which expressed well as soluble proteins. The N-  
26 terminal HaloTag fusion was found to enhance the expression and yield of FGF2, FGF3 and  
27 FGF7. Moreover, whereas FGF6, FGF8, FGF16, FGF17, FGF20 and FGF22 were only  
28 expressed as insoluble proteins, their N-terminal HaloTag fusion counterparts (Halo-FGFs)  
29 were soluble, and could be successfully purified. However, cleavage of Halo-FGF6, -FGF8  
30 and -FGF22 with TEV resulted in aggregation of the FGF protein. Thus, HaloTag provides a  
31 means to enhance the expression of soluble recombinant proteins, in addition to providing a  
32 chemical genetics route for covalent tagging of proteins.

33

## 34 Introduction

35 Of the 18 receptor-binding fibroblast growth factors (FGF), 15 also bind a heparan sulfate co-  
36 receptor and are classed as growth factors and morphogens. These are grouped into 5  
37 subfamilies based on their protein sequence similarity ([Itoh 2007](#); [Ornitz 2000](#)), and they  
38 regulate a myriad of processes in development, homeostasis and in some diseases ([Beenken  
39 & Mohammadi 2009](#); [Turner & Grose 2010](#)). Recombinant FGFs provide a key tool to study  
40 their structure-function relationships and labelling FGFs for microscopy has been important  
41 in probing the mechanisms of, for example, their transport ([Duchesne et al. 2012](#); [Lin 2004](#);  
42 [Yu et al. 2009](#)). Chemical labeling has disadvantages compared to genetically encoded  
43 labelling, since with the latter it is easier to predict the structural and hence functional  
44 consequences of labeling, which can be achieved both *in vitro* and *in vivo*. While fluorescent  
45 proteins remain a mainstay of genetic labelling, they have limitations. These have been  
46 overcome, for example, by non-covalent tagging of proteins on hexahistidine sequences with  
47 Tris-Ni<sup>2+</sup> nitriloacetic acid ([Huang et al. 2009](#); [Lata et al. 2005](#); [Tinazli et al. 2005](#)), which  
48 has allowed diverse labelling strategies, ranging from fluorescent dyes ([Uchinomiya et al.  
49 2009](#)) and quantum dots ([Roullier et al. 2009](#); [Susumu et al. 2010](#)) to gold nanoparticles  
50 ([Duchesne et al. 2008](#)). However, non-covalent coupling is reversible and exchange may  
51 occur in this instance with histidine-rich patches on endogenous proteins.

52 HaloTag is a mutant of a bacterial haloalkane dehalogenase, which reacts with chloroalkane  
53 ligands to form a covalent bond that represents the covalent intermediate of the enzyme's  
54 normal catalytic cycle ([Los et al. 2008](#)). Fluorescent dyes ([Los et al. 2008](#)) and quantum dots  
55 ([Zhang et al. 2006](#)) carrying a chloroalkane group have been used to label HaloTag fusion  
56 proteins for fluorescence imaging. This approach is particularly versatile, since it combines  
57 the power of a genetically encoded tag (the HaloTag protein) with covalent labeling.

58 Consequently, we set out to produce N-terminal HaloTag fusions of different FGFs. In the  
59 course of this work, we observed that the N-terminal HaloTag fusion had a substantial effect  
60 on the expression of the more recalcitrant FGFs, consistent with the observation that HaloTag  
61 is a potential solubilisation tag for recombinant proteins ([Ohana et al. 2009](#)). Thus, whereas  
62 expression of FGF1 and FGF10 was somewhat reduced and that of FGF2 increased,  
63 expression of FGF7, which can be toxic ([Ron et al. 1993](#)) was no longer so, while expression  
64 of soluble FGF3, FGF6, FGF7, FGF8, FGF16, FGF17, FGF20 and FGF22 was markedly  
65 enhanced. This is in contrast to previous reports where FGFs such as FGF6 ([Pizette et al.  
66 1991](#)), FGF8 ([Loo & Salmivirta 2002](#); [Macarthur et al. 1995](#); [Vogel et al. 1996](#)), FGF16  
67 ([Danilenko et al. 1999](#)) and FGF20 ([Jeffers et al. 2002](#); [Kalinina et al. 2009](#)), have been found  
68 to be mainly expressed in inclusion bodies, even as truncated proteins, and so require  
69 refolding. Thus, HaloTag provides not just a means to label proteins covalently and  
70 specifically, but is also a useful solubilisation partner for the production of recombinant  
71 proteins.

## 72 **Materials and Methods**

### 73 **Materials**

74 pET-14b vectors containing cDNAs encoding FGF1 and FGF2 and pET-M11 vector  
75 containing FGF7 cDNA were as described ([Xu et al. 2012](#)); cDNAs encoding FGF3, FGF10,  
76 FGF16, FGF17 and FGF20 were purchased from Eurofins Genomics (Ebersberg, Germany);  
77 cDNAs encoding FGF6, FGF8 and FGF22 were purchased from Life Technologies (Paisley,  
78 UK); cDNAs encoding HaloTag was acquired from Kazusa DNA Research Institute  
79 (Kisarazu, Japan); Primers for PCR were from Life Technologies. All of the protein  
80 sequences corresponding to the above cDNAs are listed in Table 1. Enzymes for cloning  
81 were from: NcoI, BamHI and T4 ligase (NEB, Hitchin, UK); KOD Hot Start DNA  
82 polymerase (Merck, Hertfordshire, UK); In-Fusion® HD Cloning Kit (Clontech, Takara Bio  
83 Europe SAS, Saint-Germain-en-Laye, France). Bacterial cells: DH5 $\alpha$ , BL21 (DE3) pLysS  
84 and SoluBL21 were a gift from Olga Mayans, University of Liverpool. The sources of other  
85 materials were as follows: LB broth and LB agar (Merck, Hertfordshire, Germany); Soniprep  
86 150 Plus (MSE, UK); Affi-Gel® Heparin Gel (Bio-Rad, Hertfordshire, UK), CM Sepharose  
87 Fast Flow, DEAE Sepharose Fast Flow, HiTrap Q HP column; empty disposable PD-10  
88 Columns; ÄKTApurifier 100 plus (GE Healthcare, Buckinghamshire, UK).

### 89 **DNA cloning of hexahistidine tagged FGFs (His-FGFs) and HaloTag tagged FGFs** 90 **(Halo-FGFs)**

91 DNA encoding FGF1, FGF3, FGF6, FGF8, FGF10, FGF16, FGF17, FGF20 and FGF22 were  
92 cloned into pET-M11 such that the protein would have an N-terminal 6xhis tag followed by a  
93 and a tobacco etch virus (TEV) cleavage site (ENLYFQ). FGF2 and FGF7 DNA sequences  
94 were previously cloned into pET-14b and pET-M11 ([Xu et al. 2012](#)).

95 A plasmid encoding Halo-FGF2 was produced by adding a HaloTag encoding DNA sequence  
96 in-frame 5' to a DNA sequence encoding full-length FGF2. This construct was then used to  
97 produce the other DNAs encoding Halo-FGFs (Figure 1). The plasmid pET-14b-*fgf2* contains  
98 NcoI and BamHI cleavage sites 5' and 3' of *fgf2*, respectively. This vector was linearized by  
99 digestion with NcoI. The DNA encoding HaloTag (Figure 1: blue insert) was amplified by  
100 PCR using the Halo-FGF2-Forward, AAGGAGATATACCATGCCAGAAATCGGTACTG,  
101 and Halo-FGF2-Reverse, TCCCGGCTGCCATGGAGCTCTGAAAGTACAGATC, primers  
102 (NcoI and BamHI cleavage sites underlined), and inserted into the linearized vector using In-  
103 Fusion enzyme. A TEV cleavage site (Figure 1: green ellipsoid) was also included at the C-  
104 terminus of HaloTag to allow release of FGF. A NotI cleavage site was also inserted 5' of the  
105 BamHI to provide an additional 3' cleavage sites for cloning. The other cDNAs (FGF1, FGF3,  
106 FGF6, FGF7, FGF8, FGF10, FGF16, FGF17, FGF20 and FGF22) were exchanged into the  
107 established pET-14b-*Halo-fgf2* plasmid by double-digestion with NcoI and BamHI/NotI  
108 enzymes and ligation using T4 ligase (Figure 1).

109

110

## 111 **Protein expression and purification of His-FGFs and Halo-FGFs**

112 His-FGF7, because it is toxic like native FGF7 ([Sher et al. 2003](#)), was transformed into BL21  
113 (DE3) pLysS for subsequent protein expression and purification. FGF2, the other His-FGFs  
114 and Halo-FGFs were transformed into SoluBL21. The bacteria containing FGF encoding  
115 plasmids were cultured at 37°C until the OD600 values were between 0.4 and 0.6, and then  
116 protein expression at 16°C was induced by adding 1 mM isopropyl β-D-1-  
117 thiogalactopyranoside (IPTG). The bacteria were harvested by centrifugation at 4°C, 14,000  
118 g for 10 minutes and the pellets frozen at -80°C.

119 The bacterial pellets were resuspended with the corresponding 50 mM Tris-Cl lysate buffers  
120 (pH 7.4) (Table 2), and the cells were disrupted by 5-6 cycles of sonication (30 s sonication,  
121 60 s pause) on ice. Cell debris and insoluble proteins were removed by centrifugation at 4°C,  
122 30,000 g for 30 minutes. Then, the presence of soluble FGFs was tested by analysis of whole  
123 cells, the supernatant and pellet by separation of polypeptides on 12% (w/v) SDS-PAGE and  
124 coomassie staining.

125 FGF2 and His-FGF7 were purified as described before ([Xu et al. 2012](#)). Soluble FGF1, FGF2,  
126 FGF3, FGF10, FGF16 and FGF17, including His-FGFs and Halo-FGFs, were loaded onto a 3  
127 mL and the other soluble FGFs were loaded onto an 8 mL column of heparin agarose. For  
128 each FGF, different concentrations of NaCl were used for washing and elution (Table 2) by  
129 following the previous measurements on the electrolyte sensitivity of their heparin binding  
130 assessed by Western blot ([Asada et al. 2009](#)), all in 50 mM Tris-Cl buffer (pH 7.4). The  
131 yields of His-FGFs and Halo-FGFs were quantified by measuring the absorbance at 280 nm  
132 and the level of impurities were estimated by analysis of coomassie stained SDS-PAGE gels  
133 with ImageJ-Analyze-Gels ([Ferreira & Rasband 2012](#)). The soluble His-FGFs eluted from  
134 heparin affinity chromatography were further purified by Ni<sup>2+</sup> affinity chromatography. Due  
135 to the negative charge on the surface of HaloTag and positive charge on the surface of FGFs,  
136 Halo-FGFs could bind to both cation- and anion-exchange stationary phases. Thus, Halo-  
137 FGF1, Halo-FGF2, Halo-FGF3, Halo-FGF7 and Halo-FGF10 were purified by  
138 chromatography on a 5 mL HiTrap Q HP column. Samples were applied in 0.15 M NaCl in  
139 PB buffer (2.7 mM KCl, 10 mM Na<sub>2</sub>HPO<sub>4</sub>, 1.8 mM KH<sub>2</sub>PO<sub>4</sub>, pH 7.4) and eluted with a  
140 gradient running to 0.8 M NaCl in the same buffer. Halo-FGF6 and Halo-FGF20 were  
141 purified by chromatography on a 3 mL column of CM Sepharose Fast Flow followed by a 3  
142 mL column of DEAE Sepharose Fast Flow. Samples were again applied in 0.15 M NaCl in  
143 PB buffer and eluted with 0.4 M NaCl in the same buffer. The purified His-FGFs and Halo-  
144 FGFs were analysed by 12% (w/v) SDS-PAGE followed by coomassie staining.

## 145 **Purification of FGFs by removing HaloTag from Halo-FGFs**

146 To test the accessibility of the TEV cleavage site, some Halo-FGFs, including Halo-FGF2,  
147 Halo-FGF17, Halo-FGF6, Halo-FGF8 and Halo-FGF22 eluted with high concentration of  
148 NaCl in 50 mM Tris buffer from heparin agarose chromatography and Halo-FGF20 purified  
149 with heparin, DEAE and CM chromatographies, were incubated with 2.5% (mol/mol) TEV  
150 protease at 4 °C overnight. In cases where the digestion products were cloudy, they were

151 clarified by centrifugation for 30 min at 13,000 g, 4 °C. Samples were then analysed on a 12%  
152 (w/v) SDS-PAGE. The supernatants of the TEV digestions of Halo-FGF6 and of Halo-  
153 FGF20 were applied onto a 2 mL heparin agarose column, and washed as before (Table 2).  
154 FGF6 and FGF20 were eluted with 1 M NaCl in PB buffer and 0.1 M arginine, 1 M NaCl in  
155 PB buffer, respectively. After TEV digestion, FGF17 was further purified on a 1 mL HiTrap  
156 SP HP cation-exchange column by washing and eluting with 0.3 M NaCl and 1 M NaCl in 50  
157 mM Tris-Cl buffer (pH 7.4). All of the fractions from the purification steps were analysed by  
158 12% (w/v) SDS-PAGE.

159

## 160 **Results and Discussion**

### 161 **Expression of soluble FGFs**

162 Based on their relative expression and solubility properties, the FGFs were split into three  
163 different groups: FGFs that expressed well as soluble proteins (FGF1, FGF2 and FGF10),  
164 FGFs that expressed at a low level, FGF3 and FGF7, and FGFs that were insoluble when  
165 expressed in *E. coli* (FGF6, FGF8, FGF16, FGF17, FGF20 and FGF22).

#### 167 **Group 1: soluble FGFs**

168 After induction, bands corresponding to the expected molecular size of His-FGF1, FGF2 and  
169 His-FGF10 were apparent in the whole cell lysates (Figs 2 A, C and E, lane L, green arrow).  
170 His-FGF1 and His-FGF10 were expressed at a higher level than FGF2 in *E. coli* SoluBL21.  
171 After centrifugation of the cell lysates, bands corresponding to the molecular size of all three  
172 FGFs were mainly recovered in the soluble fraction, rather than in the pellet (Figs 2 A, C, E,  
173 lanes S and P). Chromatography of the supernatants on heparin demonstrated that little  
174 expressed protein was present in the flow-through fraction (Figs 2 A, C, E, lane T). Weak  
175 bands corresponding to His-FGF1 and His-FGF10, but not FGF2, were observed in the wash  
176 fraction (Figs 2 A, E, lane Wa), which may represent aggregated or less well-folded protein.  
177 The major proportion of the three FGFs was recovered in the high NaCl eluate (Figs 2 A, C  
178 and E, lane Hep), which indicated that these soluble FGFs bound heparin strongly and so  
179 were likely to be properly folded, because the canonical, highest affinity heparin binding site  
180 of FGFs depends on the tertiary structure of the proteins ([Xu et al. 2012](#)).

181 The bands corresponding to Halo-FGF1, Halo-FGF2 and Halo-FGF10 were clearly observed  
182 in the whole cell lysates and these proteins were all highly expressed in SoluBL21 cells (Figs  
183 2 B, D and F, lane L, red arrow). Similarly to the His-FGF1, FGF2 and His-FGF10, after  
184 centrifugation of the whole cell lysates, the bands corresponding to the three Halo-FGFs were  
185 observed in the soluble fractions (Figs 2 B, D and F, lane S and P). Chromatography of the  
186 soluble fractions on heparin indicated that most of Halo-FGF2 and Halo-FGF10 had bound  
187 to the column, but there was a substantial amount of Halo-FGF1 in the flow-through (Fig 2 B,  
188 D and F, lane T). This may be due to the capacity of the column for Halo-FGF1 being lower  
189 than for His-FGF1. All three Halo-FGFs were eluted from the heparin affinity column at the  
190 expected NaCl concentration (Figs 2 B, D and F, lane Hep).

191 The yield of Halo-FGF1 and Halo-FGF10 was similar to that of the corresponding his-tagged  
192 proteins (Table 3). However, since the Halo-FGF proteins are considerably larger than the  
193 corresponding His-tagged FGF1 and FGF10, this represents a decrease in the molar amounts  
194 of FGF produced. In contrast, the yield of Halo-FGF2 was 4-fold higher (Table 3), which is  
195 only partly accounted for by the increased size of the fusion protein. The low yield of full-  
196 length FGF2 has been ascribed to the presence of secondary structure at the 5' end of the  
197 FGF2 mRNA ([Knoerzer et al. 1989](#)), and the presence of the upstream HaloTag sequence  
198 may mitigate this effect.

199

200



## 201 **Group 2: low expression proteins**

202 The expression of His-FGF3 was weak, as was that of His-FGF7 (expressed in BL21 DE3  
203 pLysS) due to its toxicity ([Ron et al. 1993](#)) (Figs 3A and C, lane L, S and P, green arrow).  
204 Heparin chromatography of the supernatants demonstrated that the yields of soluble His-  
205 FGF3 and His-FGF7 were quite low (Figs 3 A and C, lane Hep; Table 3).

206 Transformation of SoluBL21 with the plasmid encoding Halo-FGF7 yielded the expected  
207 number of colonies, indicating that the fusion protein was not toxic. Bands corresponding to  
208 the molecular size of Halo-FGF3 and Halo-FGF7 were observed in the cell lysates (Figs 3 B  
209 and D, lane L, red arrow) and in the soluble fraction obtained after centrifugation, whereas  
210 the pellet has relatively weaker bands (Figs 3 B and D, lanes P and S), indicating that Halo-  
211 FGF3 and Halo-FGF7 were soluble. Heparin chromatography of the soluble fractions  
212 demonstrated that large amounts of Halo-FGF3 and Halo-FGF7 retained their heparin  
213 binding interaction with the polysaccharide (Figs 3 B and D, lane Hep).

214 The yields of Halo-FGF3 and of Halo-FGF7 were 21-fold and 9-fold greater than of the  
215 corresponding His-tagged FGF (Table 3). Thus, the presence of the HaloTag N-terminal  
216 fusion increased the amounts of FGF3 and FGF7 substantially, even after taking into account  
217 the larger size of these fusion proteins (Table 3).

## 218 **Group 3: insoluble proteins**

219 His-FGF6, His-FGF8, His-FGF22, His-FGF17, His-FGF16 and His-FGF20 were all  
220 expressed, albeit at different levels. After centrifugation, bands corresponding to the  
221 molecular sizes of these proteins were detected in the pellet (Fig 4, compare lanes P and S,  
222 green arrow). Although small amounts of protein, such as bands corresponding to His-FGF6,  
223 His-FGF16 and His-FGF20, were observed in the supernatants (Fig. 4, lanes S), no protein  
224 were detected in the eluate from heparin chromatography, which might suggest these proteins  
225 were either small soluble aggregates or not properly folded. It has reported that FGF20 could  
226 also be solubilised by high concentrations of arginine ([Maity et al. 2009](#)), which suggests that  
227 FGF20 in the lysis buffer has a tendency to aggregate. Arginine would compete for binding  
228 of FGFs to heparin, however, which reduces the utility of this approach to solubilisation.

229 As illustrated by SDS-PAGE, all of the bands corresponding to the molecular size of Halo-  
230 FGF6, Halo-FGF8, Halo-FGF22, Halo-FGF17, Halo-FGF16 and Halo-FGF20 were clearly  
231 observed in the whole lysates, which suggested that all six proteins expressed well in *E. coli*  
232 (Fig. 5, lanes L, red arrow), particularly Halo-FGF6, Halo-FGF17, Halo-FGF16 and Halo-  
233 FGF20. Although some material corresponding to the expected molecular size of these Halo-  
234 FGFs was observed in the pellet after centrifugation of the cell lysates (Fig. 5, lanes P), there  
235 were strong bands corresponding to Halo-FGF6, Halo-FGF16 and Halo-FGF20 and weak  
236 bands corresponding to Halo-FGF8, Halo-FGF17 and Halo-FGF22 present in the soluble  
237 fractions (Fig. 5, lanes S). Following application to a heparin affinity column, most of Halo-  
238 FGF6 in the supernatant bound to heparin and was eluted by 1 M NaCl in Tris-Cl Buffer (Fig  
239 5 A, lane S, T and Hep). Halo-FGF8 Halo-FGF17 and Halo-FGF22 also bound to the  
240 heparin-affinity column reasonably efficiently, whereas a considerable amount of Halo-



241 FGF16 and Halo-FGF20 did not bind (Figs 5 B, C, D and E, lanes S and T). All of these four  
242 proteins could be recovered from heparin chromatography with the high concentration NaCl-  
243 containing elution buffers (Table 2) (Figs 5 B, C, D and E, lane Hep). When the Halo-FGF20  
244 in the flow-through (Fig 5 F, lane T), was applied to a second heparin-affinity  
245 chromatography column, a large amount of Halo-FGF20 was found to bind and could be  
246 eluted (Fig 5 F, lane Hep2). A considerable amount of Halo-FGF16 also failed to bind to the  
247 heparin affinity column (Fig 5 E, lane T), though the bound protein was eluted with NaCl  
248 (Fig 5 E, lane Hep). This suggests that the capacity of the heparin affinity column for Halo-  
249 FGF20 was exceeded. The same explanation may underlie the presence of Halo-FGF16 in the  
250 flow-through fraction, though this protein was present at a slightly lower level. However,  
251 since nothing is known about the preference of either FGF16 or FGF20 for binding structures  
252 in the polysaccharide, if these were relatively rare in heparin, the column capacity might  
253 easily be exceeded. Alternatively, the Halo-FGF16 in the flow through fraction may represent  
254 protein that is in small aggregates and/or not properly folded.

255 Given that the amounts of soluble His-tagged FGF6, FGF8, FGF22, FGF17, FGF16 and  
256 FGF20 were not readily detectable, the N-terminal HaloTag fusion clearly had a major effect  
257 on the expression of soluble protein. The yield of Halo-FGF6 and Halo-FGF20 was  
258 substantial (27 mg/L and 10 mg/L, respectively, Table 3). The lower yield of Halo-FGF8,  
259 Halo-FGF16, Halo-FGF17 and Halo-FGF22 (1 mg/L to 2 mg/L, Table 3) is sufficient for  
260 many applications, including microscopy. However, the heparin affinity purification step did  
261 not produce entirely pure protein, as judged by coomassie staining (Figs 2, 3, 5).

### 262 **Purification of some Halo-FGFs**

263 Four Halo-FGFs, Halo-FGF1, Halo-FGF7, Halo-FGF6 and Halo-FGF20 were chosen to  
264 determine whether the Halo-FGFs could be easily subjected to further purification, since  
265 there was clear evidence for impurities following heparin-affinity chromatography. The  
266 eluates from heparin affinity chromatography of Halo-FGF1 and Halo-FGF7 were  
267 successfully purified by Q anion-exchange chromatography (Figs 6 A and B, lane Q), which  
268 depends on the acidic isoelectric point of the HaloTag (pI: 4.77). For Halo-FGF6 and Halo-  
269 FGF20, advantage was taken of the acidic HaloTag and positive surfaces of FGFs, to enable a  
270 two-step ion-exchange purification of the eluate from heparin-affinity chromatography, using  
271 both DEAE anion and CM cation ion-exchange chromatography (Figs 6 C and D, lane DEAE  
272 and CM). The isolated Halo-FGFs are quite pure, as is shown on the gels (Fig. 6).

### 273 **Purification of FGFs by removing HaloTag with TEV protease**

274 The inclusion of a TEV site between the sequence of the HaloTag and FGF proteins provides  
275 a means to remove the HaloTag fusion partner in those instances where the HaloTag is not  
276 required for analysis (or when it may interfere with such analyses). Halo-FGF2 was first  
277 incubated with TEV protease to test whether the fusion protein could be cleaved by TEV.  
278 SDS-PAGE of the TEV digestion product of Halo-FGF2 shows that almost all of the protein  
279 was cleaved into the 35 kDa HaloTag (Fig 7 A, red arrow) and the 18 kDa FGF2 (Fig 7 A,  
280 green arrow). Thus, the cleavage site is fully accessible to TEV protease. Both Halo-FGF17

281 and Halo-FGF20 were also well digested by TEV protease and subsequently soluble FGF17  
282 (Fig 7 B, green arrow) and FGF20 (Fig 7 C, green arrow) were purified by cation-exchange  
283 and heparin chromatography, respectively.

284 Most of FGF6 (Fig 7 D, lane W<sub>Dig</sub>, green arrow) and FGF22 (Fig 7 F, lane W<sub>Dig</sub>, green arrow)  
285 and a small proportion of FGF8 were also released from HaloTag (Figs 7 D, E and F, lane  
286 W<sub>Dig</sub> and S, red arrow), but these proteins were observed to aggregate upon cleavage. This  
287 suggested that these proteins were not very stable, at least in the buffer conditions used here,  
288 and required the HaloTag N-terminal fusion to remain soluble. The soluble FGF6 released by  
289 cleavage (Fig 7 D, lane S, green arrow) was applied to a heparin affinity column, but was  
290 observed to be concentrated at the top of the column where it formed a white aggregate. Very  
291 little protein was eluted with 1 M NaCl in PB buffer (Fig 7 D, lane E, green arrow). The  
292 disappearance of FGF8 and FGF22 in the soluble fractions after TEV digestion (Figs 7 E and  
293 F, lane S) showed that these two proteins were also not very soluble in the present buffer  
294 conditions without the HaloTag fusion partner.

## 295 **Conclusion**

296 In this study, we identified four useful properties of N-terminal HaloTag fusions for the  
297 production of FGFs: i) using the HaloTag can increase the yield of low expression FGFs, ii)  
298 the HaloTag rendered FGF7 non-toxic; iii) for the insoluble FGFs, the HaloTag enabled  
299 *E.coli* to express more soluble protein at low induction temperatures and maintain solubility  
300 during isolation and storage; iv) a consequence of the low isoelectric point of HaloTag was  
301 that anion-exchange chromatography could be used as an orthogonal step in the purification  
302 of the Halo-FGFs. However, there are clearly limitations, for example, some of the FGFs did  
303 not retain solubility following cleavage from the HaloTag. This may reflect the fact that no  
304 single solubilisation tag is a universal panacea for resolving the problems of protein  
305 expression (Ferreira & Rasband 2012). Nevertheless, because the HaloTag can enhance  
306 expression of soluble protein and provide a means to label FGF protein with different  
307 fluorescent dyes and quantum dots, e.g., (Los et al. 2008; Zhang et al. 2006) it is clearly a  
308 versatile and useful tool for these two purposes and, therefore, worthwhile exploring as a part  
309 of experimental strategy with these aims.

310

311 .

312

313 **Acknowledgements**

314 Xianqing Mao would like to thank Monika Dieterle for help with cloning Halo-FGF3.

315 **Tables**

316

317 **Table 1. Peptide sequences of FGFs, the N-terminal HisTag constructs and the N-**  
 318 **terminal HaloTag constructs.** FGF names, sequences and amino acid numbering are  
 319 according to the UniProt entry. FGF1 is an N-terminal truncated protein (Ke et al., 1990).  
 320 FGF2 does not possess a secretory signal sequence, whereas there is no signal peptide  
 321 recognised in Uniprot for FGF16 and FGF20; consequently full length protein sequence was  
 322 expressed. For all other FGFs, the protein expressed was without the Uniprot determined  
 323 secretory signal sequence. FGFx refers any one of the FGFs. TEV cleavage sites are in red.  
 324

Name	UniProt accession number	Residues in mature protein
FGF1	P05230	16-155
FGF2	P09038-2	1-155
FGF3	P11487	18-239
FGF6	P10767	38-208
FGF7	P21781	32-194
FGF8b	P55075-3	23-215
FGF10	O15520	38-208
FGF16	O43320	1-207
FGF17	O60258-1	23-216
FGF20	Q9NP95	1-211
FGF22	Q9HCT0	23-170
HisTag terminus (pET-M11)	~	MKHHHHHPMSDYDIPTT <b>ENLYFQ</b> GA-[FGFx]
HaloTag and TEV site to conjoin with FGF sequence	~	MPEIGTGFPFDPHYVEVLGERMHYVDVGPRDGT PVLFLHG NPTSSYVWRNI I PHVAPTHRCIAPDLIGMGKSDK PDLGYF FDDHVRFMDAFIEALGLEEVVLVIHDWGSALGFHWAKRNP ERVKGIAFMEFIRPIPTWDEWPEFARET <b>FQ</b> AFRTTDVGRK LIIDQNVFIEGTLPMGVVRPLTEVEMDHYREPFLNPVDRE PLWRFPNELPIAGEPANIVALVEEYMDWLHQSPVPKLLFW GTPGVLI PPAAEARLAKSLPNCKAVDIGPGLNLLQEDNPD LIGSEIARWLSTLEISGEPTT <b>EDLYFQ</b> S-[FGFx]

325

326

327 **Table 2. Concentrations of NaCl in 50 mM Tris-Cl buffer (pH 7.4) used for heparin**  
328 **affinity chromatography of FGFs.** [NaCl] for lysate is the concentration of NaCl in the  
329 sample applied to the column.  
330

Name	[NaCl] for lysate (M)	[NaCl] for wash (M)	[NaCl] for elution (M)
FGF1	0.6	0.6	1.0
FGF2	0.6	0.6	1.5
FGF3	0.3	0.6	1.0
FGF6	0.3	0.4	1.0
FGF7	0.3	0.3	1.0
FGF8	0.6	0.6	1.5
FGF10	0.6	0.6	1.0
FGF16	0.3	0.4	1.0
FGF17	0.6	0.6	1.0
FGF20	0.3	0.4	1.0
FGF22	0.6	0.8	1.5

331

332 **Table 3. Summary of the molecular sizes and yields of His-FGFs and Halo-FGFs.** The  
 333 molecular weight of the proteins was calculated from their amino acid sequence. The  
 334 concentrations and volumes of His-FGFs and Halo-FGFs recovered from heparin affinity  
 335 chromatography were measured. The impurities identified by SDS-PAGE were quantified  
 336 using ImageJ relative to the band corresponding to His-FGF and to Halo-FGF and the amount  
 337 of protein in the eluate from heparin chromatography adjusted accordingly, to provide an  
 338 estimate of the yield.

FGFs	Molecular Weight (kDa)		Yield (mg/L)	
	HisTag	HaloTag	HisTag	HaloTag
FGF1	19.1	50.9	14	16
FGF2	17.3	52.2	2.5	11
	No Tag		No Tag	
FGF3	28.2	60.0	0.5	11
FGF6	22.3	54.1	n.d. <sup>1</sup>	27
FGF7	22.2	54.0	0.6	5.6
FGF8	25.7	57.5	n.d. <sup>1</sup>	1.7
FGF10	22.7	54.5	7.7	9.3
FGF16	26.9	58.7	n.d. <sup>1</sup>	1.0
FGF17	25.8	57.6	n.d. <sup>1</sup>	1.5
FGF20	26.9	58.6	n.d. <sup>1</sup>	10
FGF22	20.5	52.3	n.d. <sup>1</sup>	2.0

339

340 <sup>1</sup>Not detected. Insufficient soluble protein for reliable quantification.

341

342 **Figure legends**

343 **Figure 1: Cloning strategy for plasmids encoding Halo-FGFs.** DNA encoding HaloTag  
344 was inserted 5' of the FGF2 coding sequence with the In-Fusion HD enzyme. Subsequently, a  
345 NotI cleavage site was added 5' to the BamHI site and other FGFs were exchanged into the  
346 plasmid using the digestion-ligation cloning method. A cartoon structure of Halo-FGF is  
347 presented in the middle of this figure.

348

349 **Figure 2: Expression and heparin affinity purification of His-FGF1, FGF2, His-FGF10,**  
350 **Halo-FGF1, Halo-FGF2 and Halo-FGF10.** Following induction of expression with IPTG,  
351 cells were lysed by sonication and the insoluble material collected by centrifugation. The  
352 supernatant was subjected to heparin-affinity chromatography and samples were then analysed  
353 by SDS-PAGE and coomassie staining. Lane M, markers; L, sonicated whole cell lysate; P,  
354 pellet following centrifugation of lysate; S, corresponding supernatant; T, unbound, flow-  
355 through fraction from heparin-affinity chromatography; Wa, wash of heparin-affinity column  
356 (Table 2); Hep, high NaCl eluate of heparin-affinity column (Table 2). Green arrows: FGF or  
357 His-FGF; red arrows: Halo-FGF.

358

359 **Figure 3: Expression and heparin binding-affinity chromatography of His-FGF3, His-**  
360 **FGF7, Halo-FGF3 and Halo-FGF7.** Following induction of expression with IPTG, cells  
361 were lysed by sonication and the insoluble material collected by centrifugation. The  
362 supernatant was subjected to heparin-affinity chromatography and samples were then analysed  
363 by SDS-PAGE and coomassie staining. Lane M, markers; L, sonicated whole cell lysate; P,  
364 pellet following centrifugation of lysate; S, corresponding supernatant; T, unbound, flow-  
365 through fraction from heparin-affinity chromatography; Hep, high [NaCl] eluate of heparin-  
366 affinity column (Table 2). Green arrows: His-FGF; red arrows: Halo-FGF.

367

368 **Figure 4: Expression test of His-FGF6, His-FGF8, His-FGF22, His-FGF17, His-FGF16**  
369 **and His-FGF20.** Following induction of expression with IPTG, cells were lysed by  
370 sonication and the insoluble material collected by centrifugation. The whole cell lysate,  
371 supernatant and pellet were analysed by SDS-PAGE and coomassie staining. Lane M,  
372 markers; L, sonicated whole cell lysate; P, pellet following centrifugation of lysate; S,  
373 corresponding supernatant. Green arrows: His-FGF.

374 **Figure 5: Expression and heparin affinity purification of Halo-FGF6, Halo-FGF8, Halo-**  
375 **FGF22, Halo-FGF17, Halo-FGF16 and Halo-FGF20.** Following induction of expression  
376 with IPTG, cells were lysed by sonication and the insoluble material collected by  
377 centrifugation. The supernatant was subjected to heparin-affinity chromatography and samples  
378 were then analysed by SDS-PAGE and coomassie staining. Lane M, markers; L, sonicated  
379 whole cell lysate; P, pellet following centrifugation of lysate; S, corresponding supernatant; T,  
380 unbound, flow-through fraction from heparin-affinity chromatography; Hep, high NaCl  
381 eluate of heparin-affinity column (Table 2). Red arrows: Halo-FGF.

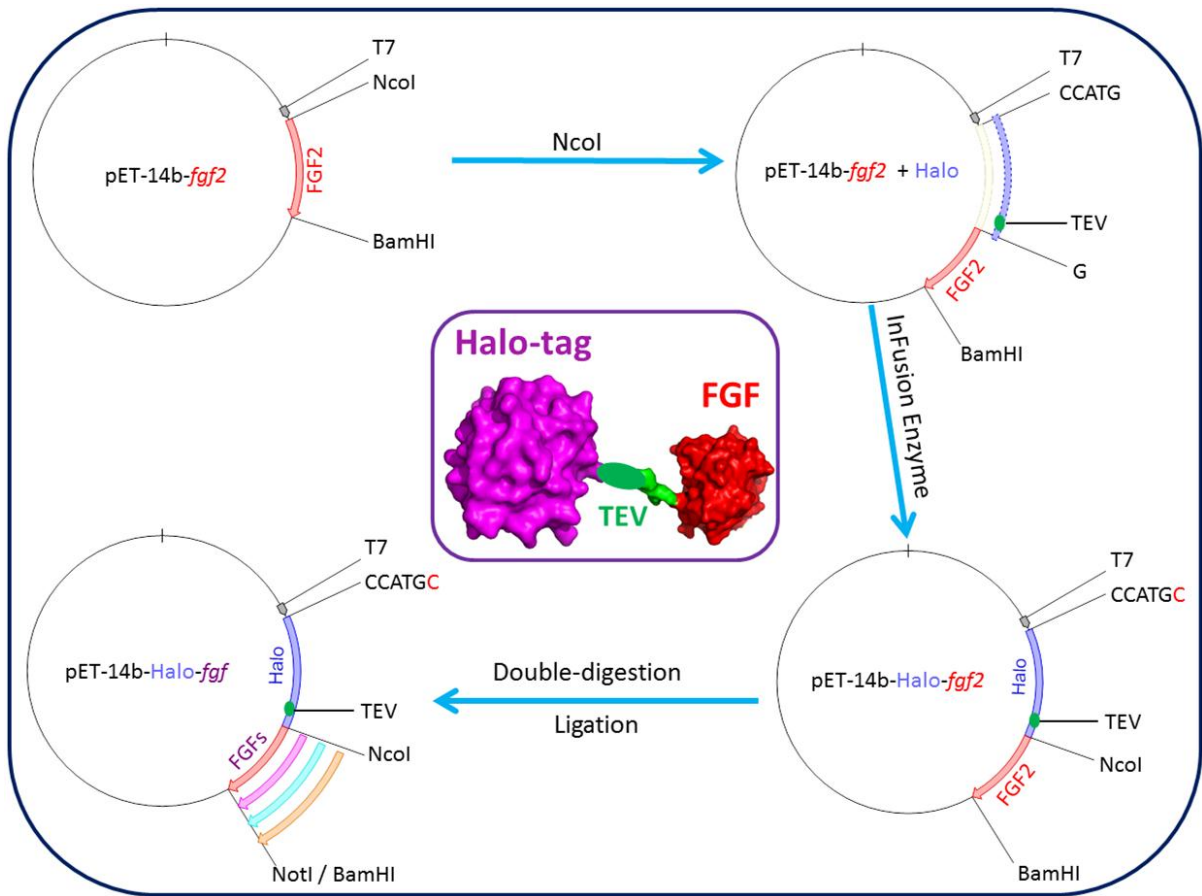
382

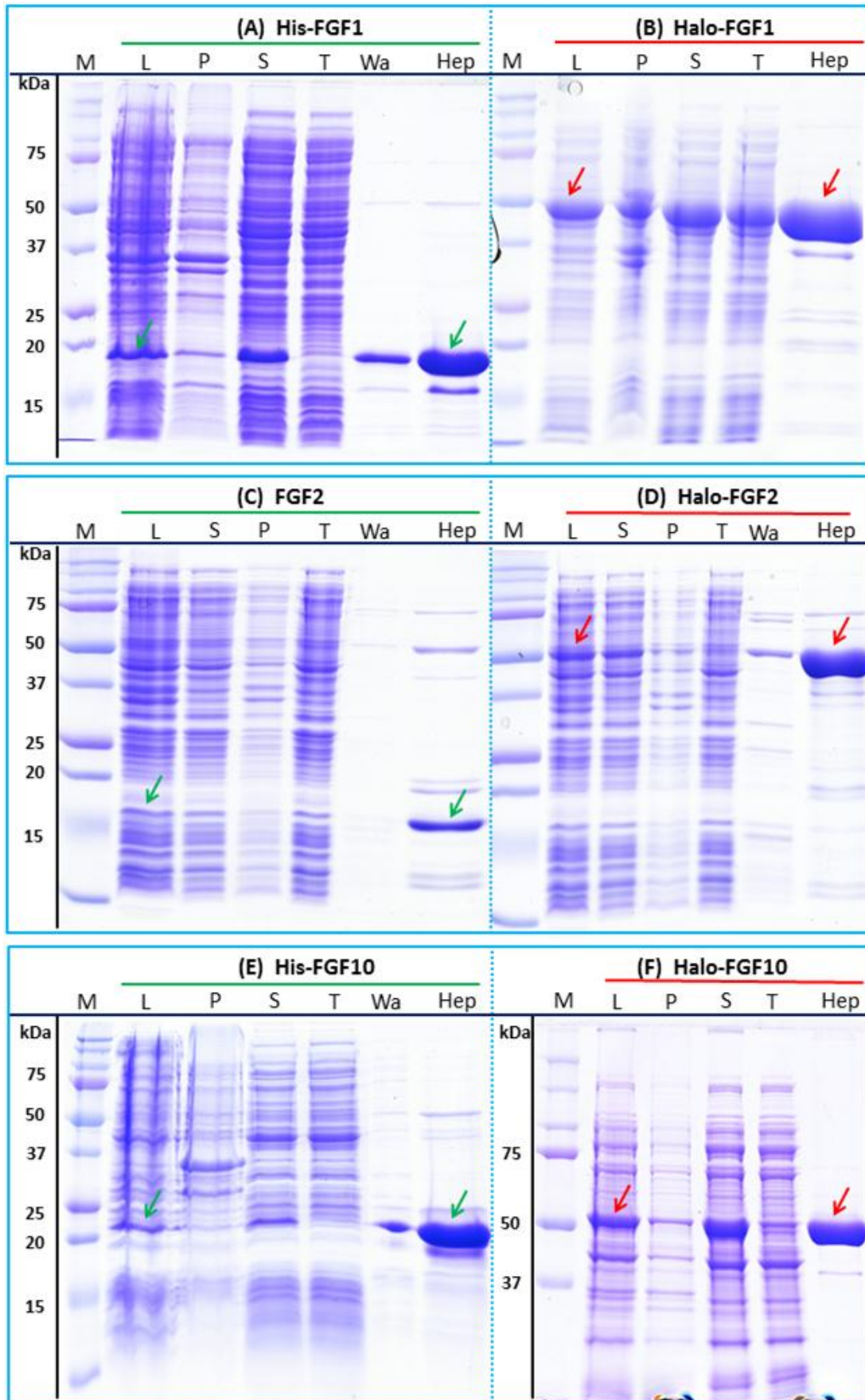


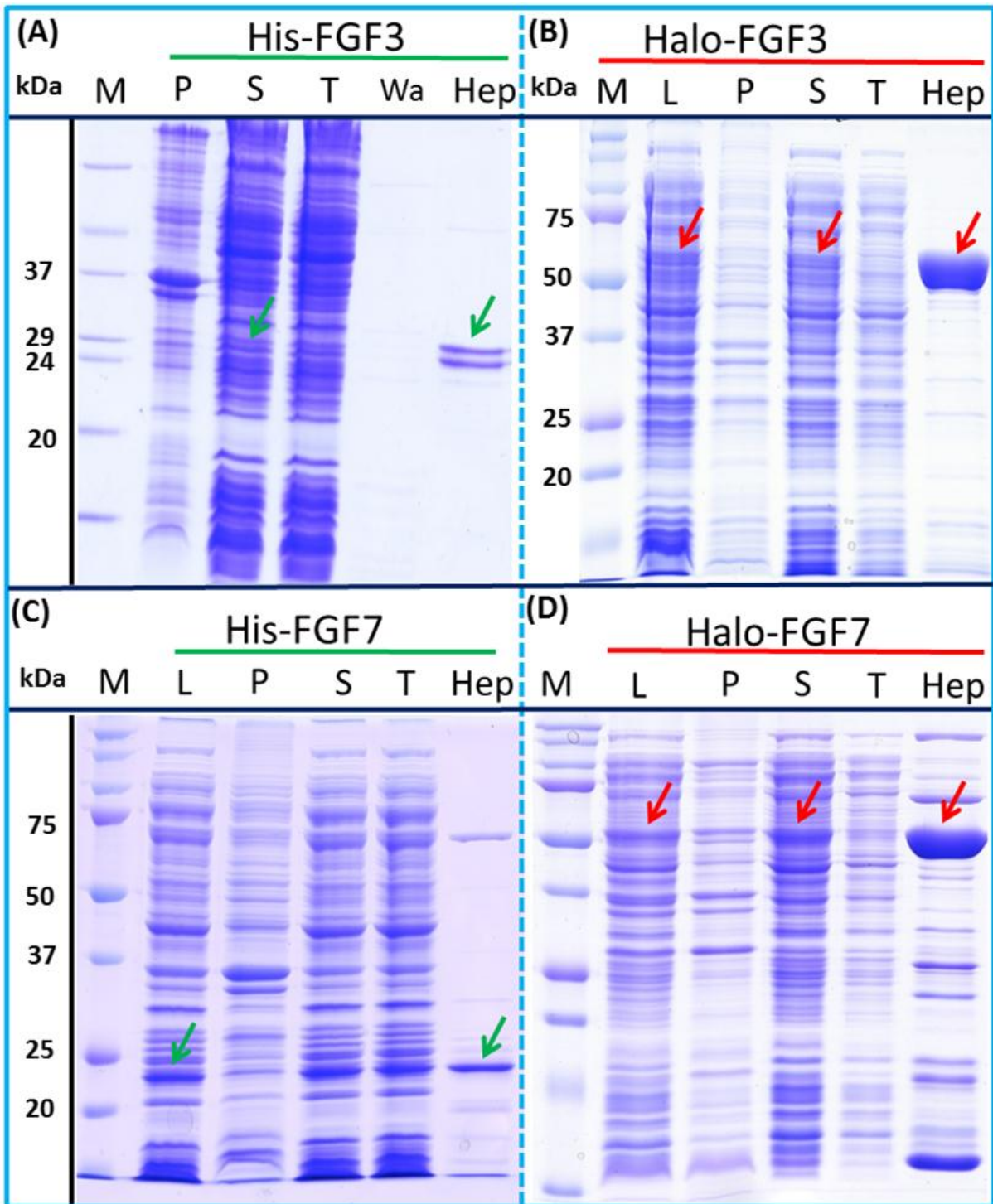
383 **Figure 6: Further purification of the heparin affinity eluate of Halo-FGF1, Halo-FGF6,**  
384 **Halo-FGF7 and Halo-FGF20 by ion-exchange chromatography.** The soluble Halo-FGF1  
385 and Halo-FGF7 eluted from heparin chromatography was purified using Q ion-exchange  
386 chromatography, while CM and DEAE ion-exchange chromatography were used to purify  
387 Halo-FGF6 and Halo-FGF20. Lane M, markers; Hep, eluate from heparin chromatography as  
388 is shown above; T, unbound, flow-through fraction from ion-exchange chromatography; Q,  
389 peak fractions collected from Q HP chromatography; DEAE eluate from DEAE  
390 chromatography, two identical samples; CM, eluate from CM chromatography. Red arrows:  
391 Halo-FGF.

392 **Figure 7: Cleavage of Halo-FGFs by TEV and purification.** The eluates of Halo-FGF2,  
393 Halo-FGF17, Halo-FGF6, Halo-FGF8 and Halo-FGF22 from heparin-affinity  
394 chromatography and the Halo-FGF20 purified by heparin and ion-exchange chromatography  
395 were digested by TEV protease to separate HaloTag and FGF. Halo-FGF6, Halo-FGF8 and  
396 Halo-FGF22 became turbid after digestion and these samples were clarified by centrifugation.  
397 Then, the samples containing FGF6 and FGF20 were subjected to heparin chromatography  
398 and that of FGF17 to SP HP cation-exchange chromatography. Lanes M, markers; Hep,  
399 eluate from heparin chromatography; W<sub>Dig</sub>, whole digestion product of Halo-FGFs purified  
400 by heparin chromatography; T, unbound, flow-through fraction from heparin chromatography;  
401 Wa, wash of SP HP cation-exchange chromatography; P, pellet following centrifugation of  
402 product of TEV digestion; S, supernatant after the centrifugation; E, high NaCl eluate of  
403 heparin or SP cation-exchange chromatography. Green arrows: FGF; red arrows: HaloTag.

404

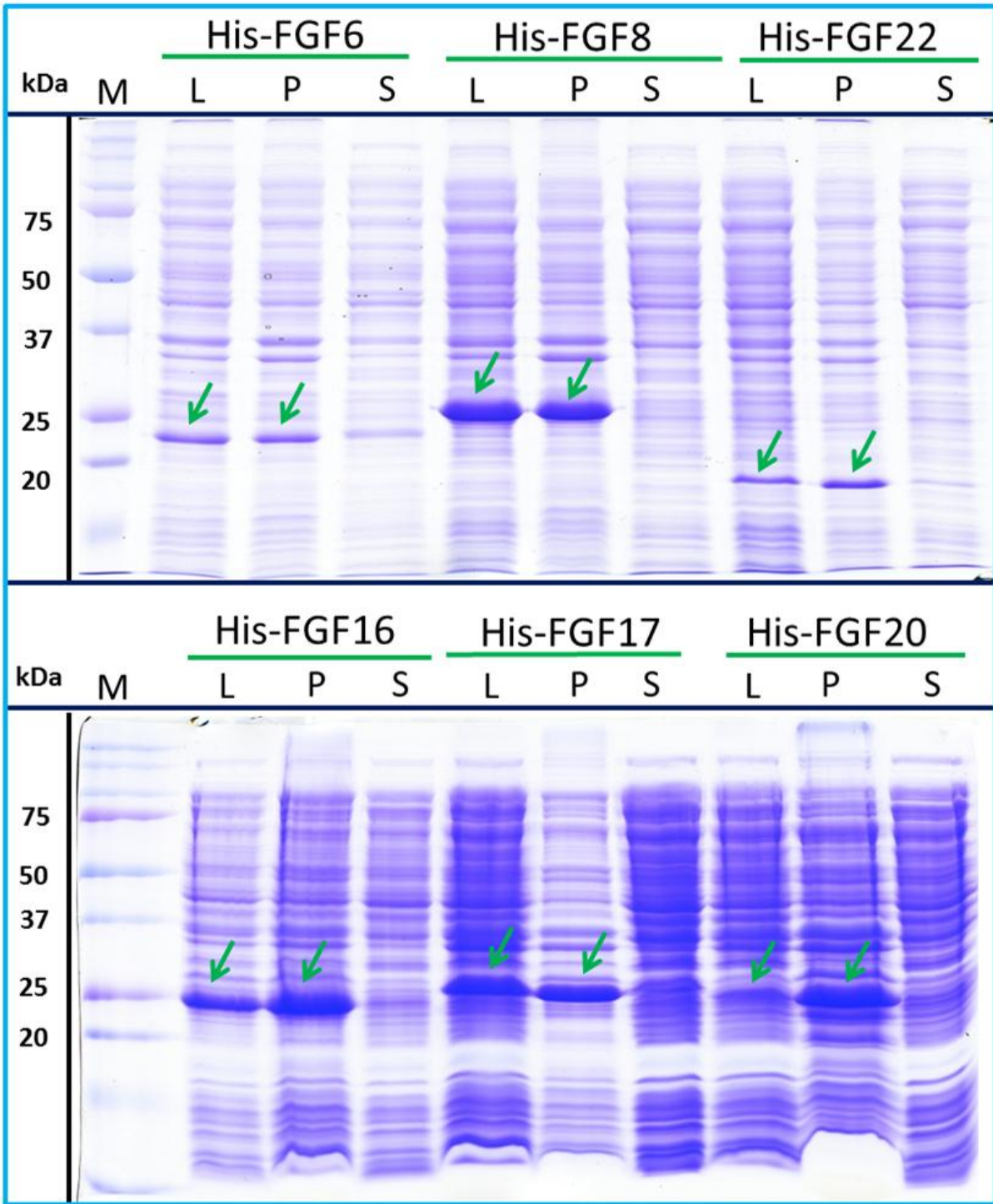


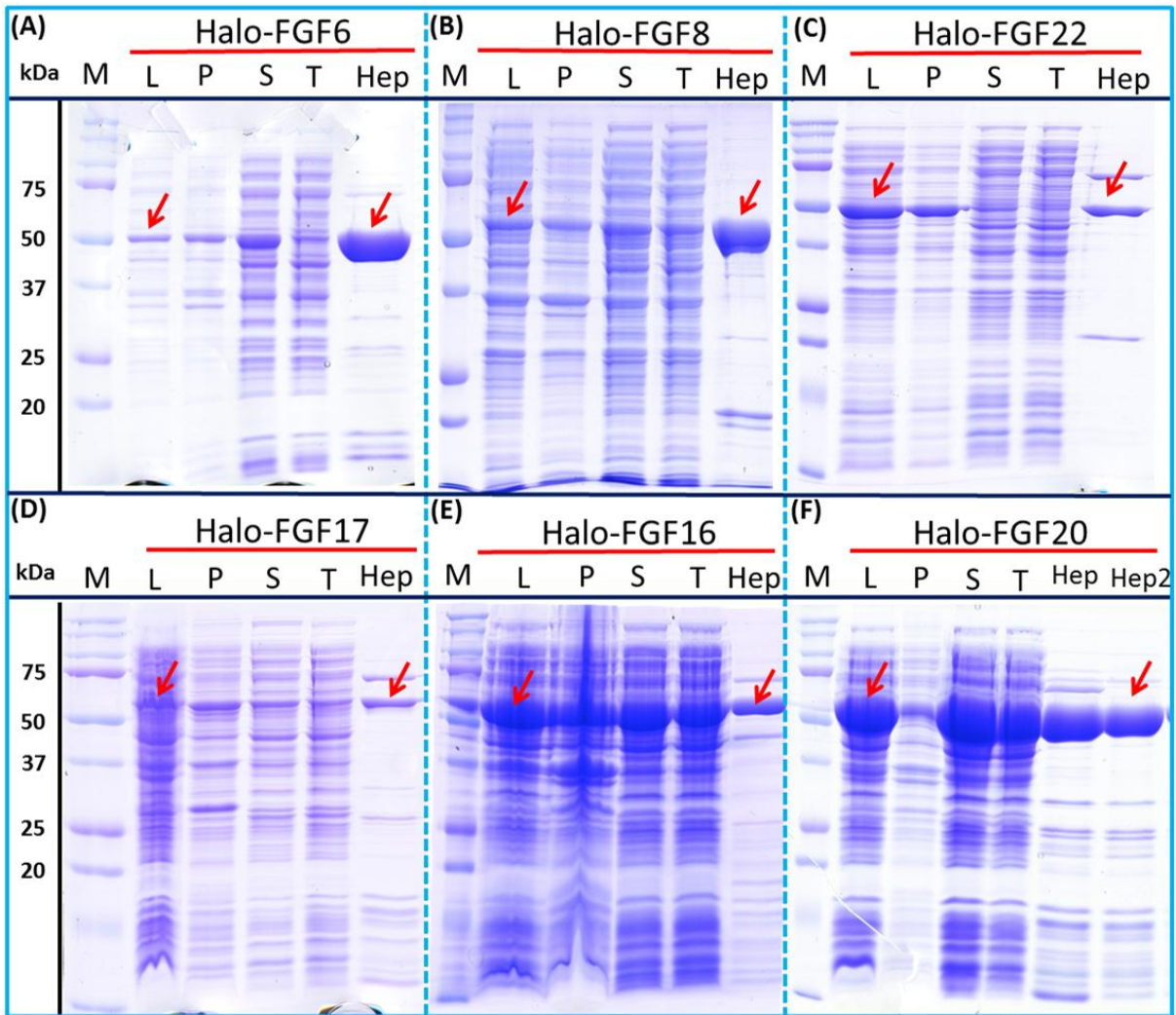


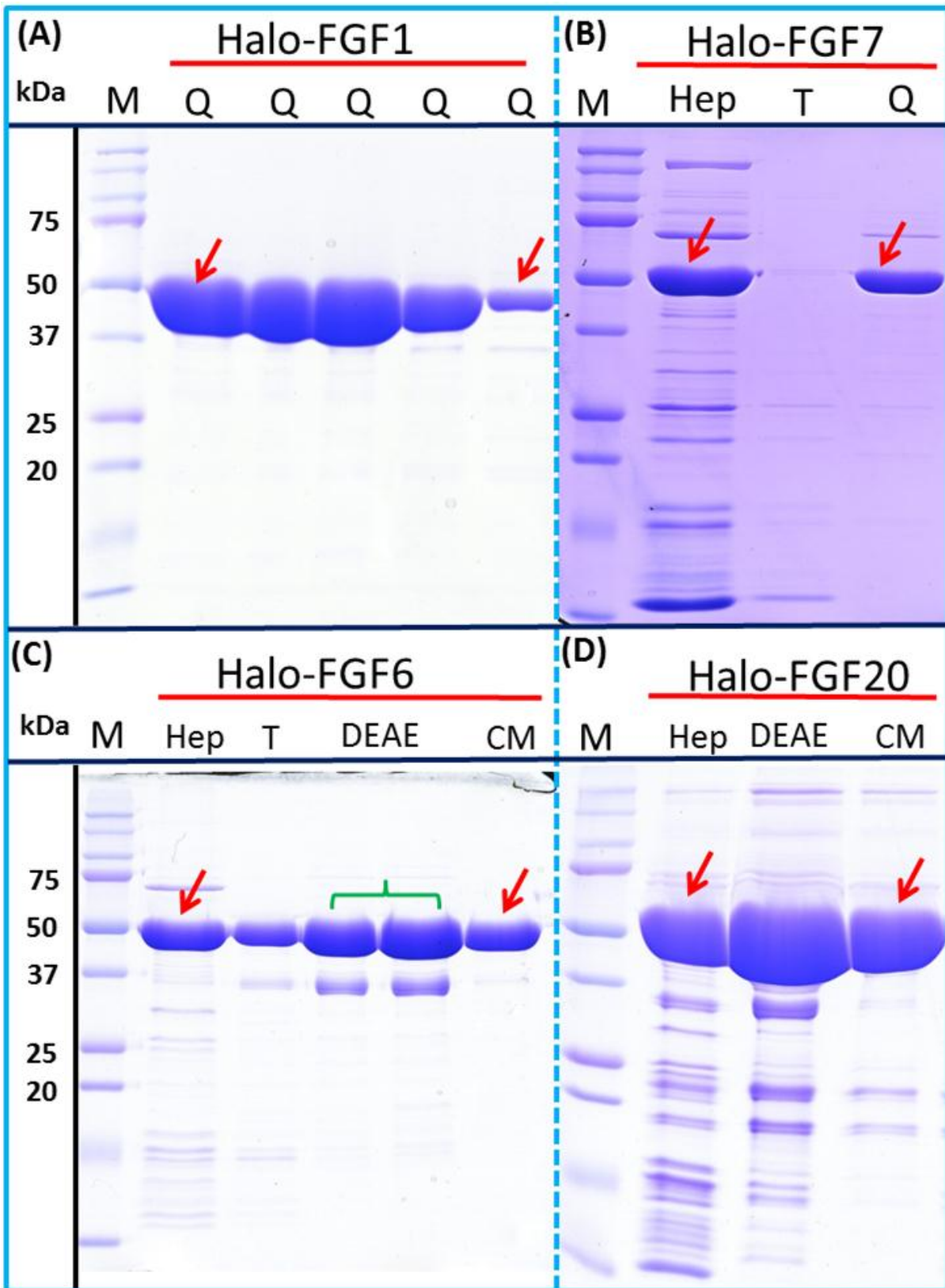


410  
411





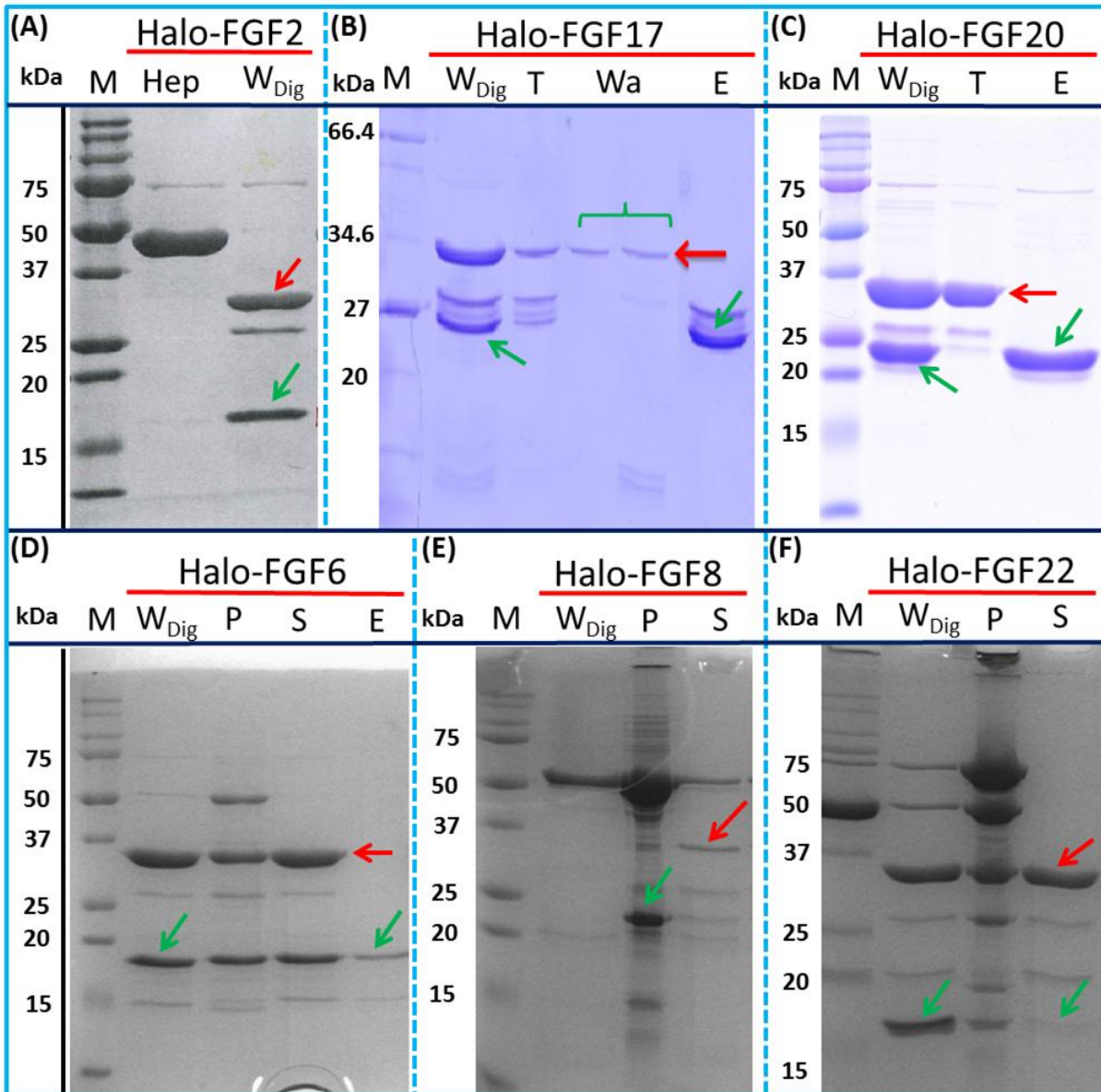




418  
 419



420 **Figure 7**



421

422

423 **References**

424

- 425 Asada M, Shinomiya M, Suzuki M, Honda E, Sugimoto R, Ikekita M, and Imamura T. 2009.  
426 Glycosaminoglycan affinity of the complete fibroblast growth factor family. *Biochimica Et*  
427 *Biophysica Acta-General Subjects* 1790:40-48.
- 428 Beenken A, and Mohammadi M. 2009. The FGF family: biology, pathophysiology and therapy. *Nature*  
429 *Reviews Drug Discovery* 8:235-253.
- 430 Danilenko DM, Montestruque S, Philo JS, Li TS, Hill D, Speakman J, Bahru M, Zhang MS, Konishi O,  
431 Itoh N, Chirica M, Delaney J, Hernday N, Martin F, Hara S, Talvenheimo J, Narhi LO, and  
432 Arakawa T. 1999. Recombinant rat fibroblast growth factor-16: Structure and biological  
433 activity. *Archives of Biochemistry and Biophysics* 361:34-46.
- 434 Duchesne L, Gentili D, Comes-Franchini M, and Fernig DG. 2008. Robust ligand shells for biological  
435 applications of gold nanoparticles. *Langmuir* 24:13572-13580.
- 436 Duchesne L, Oceau V, Bearon RN, Beckett A, Prior IA, Lounis B, and Fernig DG. 2012. Transport of  
437 fibroblast growth factor 2 in the pericellular matrix is controlled by the spatial distribution of  
438 its binding sites in heparan sulfate. *Plos Biology* 10.
- 439 Ferreira T, and Rasband W. 2012. ImageJ user guide - Analyze - Gels. Available at  
440 <http://rsbweb.nih.gov/ij/docs/guide/146-30.html#toc-Subsection-30.13> (accessed 09  
441 December 2014).
- 442 Huang ZH, Hwang P, Watson DS, Cao LM, and Szoka FC. 2009. Tris-nitrilotriacetic acids of  
443 subnanomolar affinity toward hexahistidine tagged molecules. *Bioconjugate Chemistry*  
444 20:1667-1672.
- 445 Itoh N. 2007. The FGF families in humans, mice, and zebrafish: Their evolutionary processes and roles  
446 in development, metabolism, and disease. *Biological & Pharmaceutical Bulletin* 30:1819-  
447 1825.
- 448 Jeffers M, McDonald WF, Chillakuru RA, Yang MJ, Nakase H, Deegler LL, Sylander ED, Rittman B,  
449 Bendele A, Sartor RB, and Lichenstein HS. 2002. A novel human fibroblast growth factor  
450 treats experimental intestinal inflammation. *Gastroenterology* 123:1151-1162.
- 451 Kalinina J, Byron SA, Makarenkova HP, Olsen SK, Eliseenkova AV, Larochele WJ, Dhanabal M, Blais S,  
452 Ornitz DM, Day LA, Neubert TA, Pollock PM, and Mohammadi M. 2009. Homodimerization  
453 controls the fibroblast growth factor 9 subfamily's receptor binding and heparan sulfate-  
454 dependent diffusion in the extracellular matrix. *Molecular and Cellular Biology* 29:4663-  
455 4678.
- 456 Knoerzer W, Binder HP, Schneider K, Gruss P, Mccarthy JEG, and Risau W. 1989. Expression of  
457 synthetic genes encoding bovine and human basic fibroblast growth-factors (bFGFs) in  
458 escherichia-coli. *Gene* 75:21-30.
- 459 Lata S, Reichel A, Brock R, Tampe R, and Piehler J. 2005. High-affinity adaptors for switchable  
460 recognition of histidine-tagged proteins. *Journal of the American Chemical Society*  
461 127:10205-10215.
- 462 Lin XH. 2004. Functions of heparan sulfate proteoglycans in cell signaling during development.  
463 *Development* 131:6009-6021.
- 464 Loo BM, and Salmivirta M. 2002. Heparin/heparan sulfate domains in binding and signaling of  
465 fibroblast growth factor 8b. *Journal of Biological Chemistry* 277:32616-32623.
- 466 Los GV, Encell LP, McDougall MG, Hartzell DD, Karassina N, Zimprich C, Wood MG, Learish R, Ohane  
467 RF, Urh M, Simpson D, Mendez J, Zimmerman K, Otto P, Vidugiris G, Zhu J, Darzins A,  
468 Klaubert DH, Bulleit RF, and Wood KV. 2008. HatoTag: A novel protein labeling technology  
469 for cell imaging and protein analysis. *Acs Chemical Biology* 3:373-382.
- 470 Macarthur CA, Lawshe A, Xu JS, Santosocampo S, Heikinheimo M, Chellaiah AT, and Ornitz DM. 1995.  
471 Fgf-8 isoforms activate receptor splice forms that are expressed in mesenchymal regions of  
472 mouse development. *Development* 121:3603-3613.

- 473 Maity H, Karkaria C, and Davagnino J. 2009. Effects of pH and arginine on the solubility and stability  
474 of a therapeutic protein (fibroblast growth factor 20): relationship between solubility and  
475 stability. *Current Pharmaceutical Biotechnology* 10:609-625.
- 476 Ohana RF, Encell LP, Zhao K, Simpson D, Slater MR, Urh M, and Wood KV. 2009. HaloTag7: A  
477 genetically engineered tag that enhances bacterial expression of soluble proteins and  
478 improves protein purification. *Protein Expression and Purification* 68:110-120.
- 479 Ornitz DM. 2000. FGFs, heparan sulfate and FGFRs: complex interactions essential for development.  
480 *Bioessays* 22:108-112.
- 481 Pizette S, Batoz M, Prats H, Birnbaum D, and Coulier F. 1991. Production and functional-  
482 characterization of human recombinant FGF-6 protein. *Cell Growth and Differentiation*  
483 2:561-566.
- 484 Ron D, Bottaro DP, Finch PW, Morris D, Rubin JS, and Aaronson SA. 1993. Expression of biologically-  
485 active recombinant keratinocyte growth-factor - structure-function analysis of amino-  
486 terminal truncation mutants. *Journal of Biological Chemistry* 268:2984-2988.
- 487 Roullier V, Clarke S, You C, Pinaud F, Gouzer G, Schaible D, Marchi-Artzner V, Piehler J, and Dahan M.  
488 2009. High-affinity labeling and tracking of individual histidine-tagged proteins in live cells  
489 using Ni<sup>2+</sup> Tris-nitrilotriacetic acid quantum dot conjugates. *Nano Letters* 9:1228-1234.
- 490 Sher I, Yeg BK, Mohammadi M, Adir N, and Ron D. 2003. Structure-based mutational analyses in  
491 FGF7 identify new residues involved in specific interaction with FGFR2IIIb. *Febs Letters*  
492 552:150-154.
- 493 Susumu K, Medintz IL, Delehanty JB, Boeneman K, and Mattoussi H. 2010. Modification of  
494 poly(ethylene glycol)-capped quantum dots with nickel nitrilotriacetic acid and self-assembly  
495 with histidine-tagged proteins. *Journal of Physical Chemistry C* 114:13526-13531.
- 496 Tinazli A, Tang JL, Valiokas R, Picuric S, Lata S, Piehler J, Liedberg B, and Tampe R. 2005. High-affinity  
497 chelator thiols for switchable and oriented immobilization of histidine-tagged proteins: A  
498 generic platform for protein chip technologies. *Chemistry-a European Journal* 11:5249-5259.
- 499 Turner N, and Grose R. 2010. Fibroblast growth factor signalling: from development to cancer.  
500 *Nature Reviews Cancer* 10:116-129.
- 501 Uchinomiya S, Nonaka H, Fujishima S, Tsukiji S, Ojida A, and Hamachi I. 2009. Site-specific covalent  
502 labeling of His-tag fused proteins with a reactive Ni(II)-NTA probe. *Chemical*  
503 *Communications*:5880-5882.
- 504 Vogel A, Rodriguez C, and IzpisuaBelmonte JC. 1996. Involvement of FGF-8 in initiation, outgrowth  
505 and patterning of the vertebrate limb. *Development* 122:1737-1750.
- 506 Xu RY, Ori A, Rudd TR, Uniewicz KA, Ahmed YA, Guimond SE, Skidmore MA, Siligardi G, Yates EA, and  
507 Fernig DG. 2012. Diversification of the structural determinants of fibroblast growth factor-  
508 heparin interactions implications for binding specificity. *Journal of Biological Chemistry*  
509 287:40061-40073.
- 510 Yu S, Burkhardt M, Nowak M, Ries J, Petrásek Z, Scholpp S, Schwille P, and Brand M. 2009. FGF8  
511 morphogen gradient is formed by a source-sink mechanism with freely diffusing molecules.  
512 *Nature* 461:533-536.
- 513 Zhang Y, So MK, Loening AM, Yao HQ, Gambhir SS, and Rao JH. 2006. HaloTag protein-mediated site-  
514 specific conjugation of bioluminescent proteins to quantum dots. *Angewandte Chemie-*  
515 *International Edition* 45:4936-4940.

516